

Polyethylene–Poly(ethylene oxide) Hybrid Films Obtained by Crazing and Their Structural Peculiarities

Alena Y. Yarysheva,^{*,†} Dmitry V. Bagrov,[‡] V. Artem V. Bakirov,^{§,⊥} Boris N. Tarasevich,[†] Tatiana E. Grohovskaya,[†] Larisa M. Yarysheva,[†] Sergey N. Chvalun,^{§,⊥} and Aleksandr L. Volynskii[†]

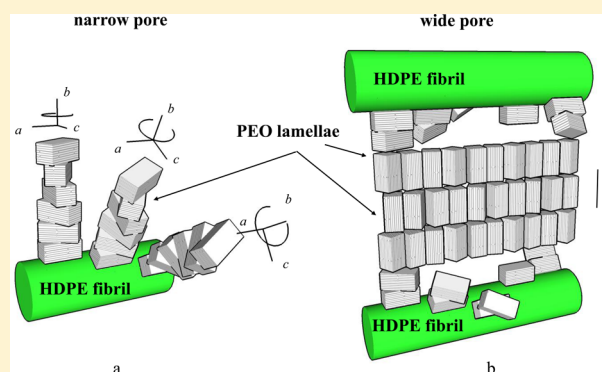
[†]Faculty of Chemistry, Lomonosov Moscow State University, Leninskie gory 1-3, Moscow 119991, Russia

[‡]Faculty of Biology, Lomonosov Moscow State University, Leninskie gory 1-12, Moscow 119991, Russia

[§]National Research Center Kurchatov Institute, Akademika Kurchatova, pl. 1, 123182, Moscow, Russia

[⊥]Institute of Synthetic Polymer Materials RAS, Profsoyuznaya st. 70, 117393, Moscow, Russia

ABSTRACT: Hybrid films have been obtained by crazing high-density polyethylene (HDPE) in a poly(ethylene oxide) (PEO) solution. Deformation by the crazing mechanism gives rise to the formation of a nanoporous structure in HDPE, with the PEO solution penetrating into it. A uniform HDPE–PEO hybrid film is obtained after the solvent is removed. The structure of crazed HDPE has been shown to govern the structure of incorporated PEO. By wide-angle X-ray scattering (WAXS), differential scanning calorimetry (DSC), and Fourier transform infrared spectroscopy (FTIR), we have found out, that PEO crystallization in HDPE film is accompanied by an orientation and a decrease in the crystallinity and melting temperature of PEO due to the spatial confinements caused by the nanoporous HDPE matrix. The revealed effects depend on the pore size, which is, in turn, determined by the degree of HDPE deformation (tensile strain). The lower the strain (HDPE pore size), the greater the decrease in the crystallinity of incorporated PEO. As the tensile strain of HDPE is increased, the orientation of PEO lamellae in the HDPE film changes and flat-on lamellae of PEO arise in addition to edge-on lamellae.



INTRODUCTION

Stretching of amorphous glassy and semicrystalline polymers in adsorptionally or plasticizing active liquids proceed by crazing mechanism. Deformation coincides with development of a nanoscale fibrillar-porous structure in the stretching polymer.^{1–3} As has been established previously,^{4–7} under certain conditions, low- and high-molecular-mass compounds dissolved in a liquid used for crazing are capable of penetrating into the nanoporous structure of deformed polymer. Removal of a volatile solvent yields a hybrid film of the matrix polymer with the substance that has penetrated into the pores with the solvent. Thus, crazing as a method of producing hybrid films is of interest for solving fundamental problems relevant to the transport of molecules into nanopores and their structuring (crystallization, orientation) in a confined nanoscale space. Crazed polymers are considered to be model systems convenient for studying these problems, because morphology and parameters of the fibrillar–porous structure of crazes may be tuned by varying deformation conditions and choice of the matrix polymer with different initial structure (polycarbonates, poly(ethylene terephthalate), poly(vinyl chloride), polyamide-6, polyamide-12, HDPE, polypropylene).^{1,2}

Polymer crystallization in confined volumes (in nanopores, template and nanolayered films, nanofibers, nanotubes) is

known to distinguish by some peculiarities. A reduction in the polymer phase volume to a few tens of nanometers leads to fundamental changes in polymer properties (a decrease in glass-transition temperature, crystallization temperature and heat, and crystallinity). Moreover, the mechanism of nucleation changes, thus leading to the formation of crystallites with different types of morphologies and orientations.^{8–18}

Spatial confinements strongly affect crystallization processes, because, being a fundamental parameter, the size of the phase nucleus plays the key role in the phase transformations of this kind.¹⁹ The typical size of a phase nucleus is from a few nanometers to several tens of nanometers; hence, the spatial confinements must primarily affect the nucleation process. In a confined space, phase nucleation prevails over phase growth, thereby leading to a decrease in the sizes of crystallites and an increase in their interfacial surface area. In accordance with the Gibbs–Thomson formula, such crystallites will melt at lower temperatures. As the size of a confinement (e.g., pore diameter) decreases, the degree of polymer crystallinity under the

Received: November 22, 2016

Revised: February 17, 2017

Published: March 24, 2017

confined conditions reduces until the polymer completely loses the ability to crystallization.²⁰

The peculiarities of polymer crystallization in a nanoscale volume are governed by the size and morphology of a “hindering” confinement, the character of the polymer–solid surface interaction, and the ratio between the rates of crystallite nucleation and growth. For example, in the case of cylindrical pores with 2D confinements in templates, nanotubes, and track membranes, both the parallel orientation of macromolecular chains relative to a pore axis, i.e., edge-on lamellae, and the perpendicular orientation of macromolecular chains with respect to the pore axis, i.e., the flat-on lamellae, may be observed.^{15,17,21–23} Thus, nanoscale confinements have a substantial effect on all characteristics and the structure of a crystallizing polymer.

The goal of this work was to use the crazing method to obtain hybrid films from polymers of different natures, such as hydrophobic HDPE and hydrophilic PEO, and to study the influence of the nanoporous structure of the matrix polymer (HDPE) on the structure of the incorporated polymer (PEO).

EXPERIMENTAL SECTION

Materials. Hybrid films were prepared using HDPE ($M_w = 210$ kDa, $M_n = 70$ kDa) films 25 μm thick (Stamylan, DSM) produced by extrusion blow molding and a 20 wt % solution of PEO (Aldrich, $M_w = 20$ kDa) in a water–ethanol (1:7, vol/vol) mixed solvent. Films with sizes of 40 \times 20 mm were subjected to planar stretching in the water–ethanol PEO solution at room temperature and a rate of 27%/min. After removing from PEO solutions the samples were wiped off in order to remove the residual PEO from their surface; then, to remove the solvent, the samples were dried under isometric conditions in air flow during 30 min at room temperature. To remove any residual solvent the samples were placed in vacuum for 1 h. The content of PEO was determined as a change in the film mass as follows: $\Delta m/m_0 = [(m_t - m_0)/m_0] \times 100$ (%), where m_0 is the mass of an initial HDPE film and m_t is the mass of the HDPE–PEO hybrid film. The mean squared deviation of PEO content was $\pm 2\%$. The theoretical content of PEO was estimated assuming that the surrounding PEO solution was merely filling the whole pore volume without any change in the concentration: $\Delta m/m_0$ (theory) = $[CW_t / (1 - W_t)\rho] \times 100\%$, with ($C = 200$ kg/m³) being the PEO solution concentration, ($\rho = 950$ kg/m³) being the HDPE density, ($W_t = \Delta V/V_t$) = volume strain of HDPE as the ratio of volume increment ΔV resulting from film stretching to sample volume under the same tensile strain.

Atomic Force Microscopy (AFM) Study. Films HDPE with sizes of 40 \times 20 mm were subjected to planar stretching in a water–ethanol solution (1:7, vol/vol) at room temperature and a rate of 27%/min. Stretched films were fastened in circular frames to prevent them from shrinkage, and the measurements were performed in the liquid medium in which the stretching had been carried out. All AFM experiments were performed using a Solver Pro-M atomic force microscope (NT-MDT, Zelenograd, Russia) in the “scanning by probe” configuration. A Smena scanning head equipped with closed-loop feedback sensors was used (scanning range was 100 \times 100 \times 7 μm). The scanning was carried out in the contact mode with MSC-T-AUHW cantilevers (Bruker, formerly Veeco, Santa Barbara, CA). The AFM images were processed using the Femtoscan online software package (Advanced Technologies Center, Russia).

Volume Strain. Volume strain (W) of the deformed polymer was calculated from the changes in the geometric sizes of the films as the ratio of volume increment ΔV resulting from film stretching to initial sample volume V_0 , $W = (\Delta V/V_0) \times 100$ (%). The geometric sizes of a deformed HDPE sample were measured with a projector operating at a 10-fold magnification and an IZV2 optimizer. The mean squared deviation of volume strain was $\pm 3\%$.

Scanning Electron Microscopy (SEM) with the X-ray Spectral Analysis. The distribution of PEO in HDPE–PEO films was studied

by a scanning electron microscope (Hitachi S-520, Japan). Prior to the SEM observations, the samples were fractured in the liquid nitrogen along to the direction of tensile stretching. The fractured surfaces were decorated with gold on an Eiko IB-3 unit by the method of ionic plasma sputtering.

Differential Scanning Calorimetry (DSC). The experiments were performed with a TA 4000 thermoanalyzer (Mettler) using samples with a mass of 1.5–2 mg. Ideal crystal melting heats, which were used to calculate the degrees of crystallinity, were 293 and 196.8 J/g for HDPE and PEO, respectively. The heating rate was 10 K/min.

FTIR Measurements. Orientation of PEO macromolecules in HDPE films was studied spectrophotometrically using a Thermo Nicolet IR200 FTIR spectrometer operating at the number of scans and a resolution of 30 and 2 cm^{-1} , respectively. The measurements were carried out in a range of 400–2000 cm^{-1} using a film IR polarizer located in the cell compartment of the instrument at parallel and perpendicular orientations of the polarization plane with respect to the direction of polymer film stretching. The quantitative analysis of polymer chain orientation can be implemented by FTIR spectroscopy using the principle of dichroism (D), which is determined as the ratio between the absorptions at parallel (A_{\parallel}) and perpendicular (A_{\perp}) incident radiation polarizations with respect to the stretching direction of HDPE film, $D = (A_{\parallel})/(A_{\perp})$.

X-ray Diffraction Analysis. The wide-angle X-ray scattering (WAXS) analysis of hybrid films was performed with a DIKSI station of the Kurchatov synchrotron (National Research Center Kurchatov Institute). A 1.7 T rotating magnet operating at a radiation power of 7.65 keV (1.625 A), resolution dE/E of 10^{-3} , and a photon flux of 10^9 was used as a source of radiation. The beam size at a sample was 0.5 \times 0.3 mm; diffraction patterns were recorded with a Dectris Pilatus 1 M detector.

RESULTS AND DISCUSSION

The Structure of Crazed HDPE. Figure 1 shows the AFM images of HDPE with initial row-structure after stretching in

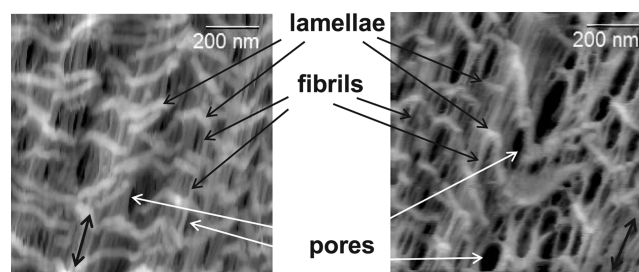


Figure 1. AFM images of HDPE stretched in the water–ethanol to strains of (a) 75 and (b) 300% along the extrusion axis (indicated by arrow).

the water–ethanol solution. HDPE deformation via the crazing mechanism is accompanied by the formation of a fibrillar–porous structure in the interlamellar space. The pores have a slitlike shape, with fibrils connecting neighboring lamellae or their stacks and being oriented along the stretching axis (Figure 1a). The comparison between images a and b in Figure 1 shows that, as the tensile strain increases, the lamellae are spread, the interlamellar distance increases, while their longitudinal sizes, on the contrary, decrease because of fragmentation. At a tensile strain of 300%, a large scatter of pore widths is observed, and rather wide pores arise in addition to narrow ones; in some places, the structure of HDPE resembles a network of fibrils, with its nodes being formed by lamella fragments.

Parameters of the porous structure were analyzed for a large number of the images, and pore size distribution curves were plotted. According to the AFM data, at a tensile strain of 75%,

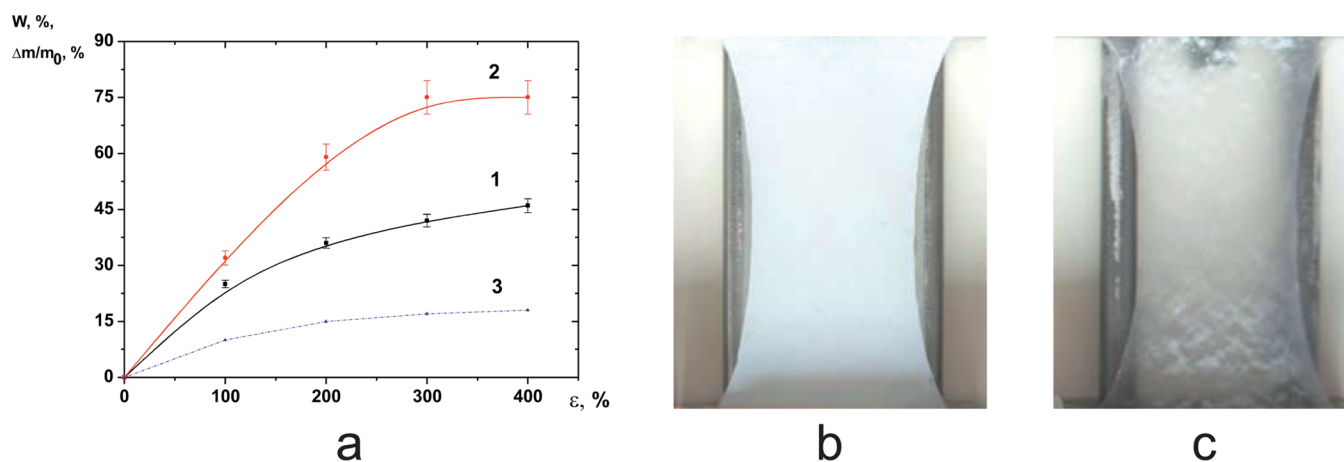


Figure 2. (a) Influence of HDPE film tensile strain ε on (1) the content of PEO with a molecular mass of 20 kDa and (2) volume strain (W). Curve 3 refers to the PEO content calculated under the assumption that its concentration in the pore volume is equal to the concentration in the solution (20%). The strain rate is 27%/min. (b, c) Photographs of HDPE samples stretched in (b) the water–ethanol and (c) the water–ethanol PEO solution by 200%. The photographs have been taken after removal of the solvent.

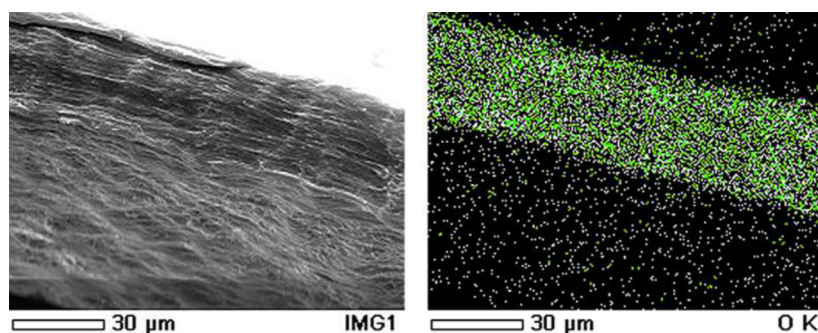


Figure 3. Distribution of oxygen atoms over a cleavage of a hybrid film resulting from 200% crazing of HDPE (with a thickness of 60 μm) in a solution of PEO with a molecular mass of 20 kDa: (a) the SEM of the cleavage and (b) the image obtained by the X-ray spectral analysis of the same cleavage. The green dots denote the distribution of oxygen.

the distance between HDPE lamellae in a pore is in a range of 30–60 nm, while the sum of the pore width and fibril diameter is 10–20 nm. It is measured as the distance between the adjacent fibrils, this parameter is less dependent on the cantilever radius than the fibril diameter. At a tensile strain of 300%, the pore length is 70–130 nm, and the sum of the pore width and fibril diameter is 15–50 nm. Thus, as the tensile strain is increased, the length and width of the pores grow and their morphology changes. The deformation of HDPE via the crazing mechanism has been considered in detail elsewhere.^{24,25}

Preparation of HDPE–PEO Hybrid Films by Means of Crazing HDPE in PEO Solutions. As has been established, PEO dissolved in water–ethanol medium used for HDPE crazing is capable of penetrating into the nanoporous structure of HDPE. Removal of a volatile liquid yields a hybrid film of the deformed HDPE and the PEO that has penetrated into the pores with the solvent.

Figure 2a presents the content of PEO in HDPE films stretched in water–ethanol PEO solutions (curve 1) and the volume strain of the films stretched in the water–ethanol (curve 2) as functions of HDPE tensile strain. It can be seen that a rise in the tensile strain leads to an increase in the volume strain and the content of PEO in the HDPE films. At high tensile strains, the PEO content in the HDPE films may exceed 45%.

The questions as to the penetration of PEO into the pores of a polymer being crazed have been considered in.⁴ Taking into account the scaling ideas,²⁶ it has been assumed that macromolecules of flexible-chain polymers penetrate into the nanoporous structure of deformed polymers as a result of reptation, with the ξ (blob size) $\leq D$ (pore diameter) relation being the key factor determining the penetration efficiency. The curve 3 in Figure 2a refers to the PEO content calculated under the assumption that its concentration in the pore volume is equal to the concentration in the solution. As is seen from the comparison between curves 1 and 3 in Figure 2a, the experimentally determined content of PEO in HDPE films appears to be substantially higher than that in the ambient solution throughout the range of deformations. Apparently, PEO is adsorbed on the surface of crazes in deformed polymers, because crazed polymers have a highly developed specific surface area as large as 100 m^2/g and are efficient adsorbents.¹

Parts b and c of Figure 2 depict the photographs of HDPE films stretched in the water–ethanol and water–ethanol PEO solutions. The crazed HDPE film has a milk-white color (Figure 2b) because of the light scattering on numerous pores. The film of the HDPE–PEO is semitransparent, thus indicating that the formed cavities are partially filled with PEO (Figure 2c).

In order to verify the uniformity of PEO distribution in HDPE films, the samples were studied by X-ray spectral microanalysis. The thicker HDPE films (60 μm) were used, as we suggested that greater thickness would have become an obstacle for uniform filling of HDPE structure. Parts a and b of Figure 3 show the micrograph of the cleavage of an HDPE film containing 35% PEO and the distribution of oxygen atoms in this cleavage, respectively. It can be seen that oxygen, which is present in PEO molecules alone and absent in initial HDPE, is uniformly distributed over the cleavage. Thus, HDPE films are filled with PEO uniformly.

The Study of HDPE–PEO Hybrid Films by Differential Scanning Calorimetry (DSC). As has been shown above, pores in crazed HDPE have a slitlike shape and are located between lamellae. As a result, the pore length is the long period (the distance between neighboring lamellae) minus the lamella thickness, while the pore width is the interfibrillar distance. The deformation is accompanied by the spreading and fragmentation of lamellae, shifts of lamella fragments relative to each other, and thinning of fibrils; therefore, the pore size increases with the tensile strain (Figure 1). However, even at the highest tensile strains (as high as 400%), the pore width in HDPE is no larger than 100 nm.²⁴ Thus, when the solvent is removed, PEO crystallizes under the conditions of the confined nanoscale pore space.

In this work, DSC was employed to study the initial HDPE films, PEO homopolymer with a molecular mass of 20 kDa, and HDPE–PEO films obtained at different tensile strains of HDPE. The works devoted to the structure formation under “hindered” conditions are, as a rule, dealing with crystallization processes. This work is distinguished by the fact that a polymer crystallizes in a matrix, which represents a system of interconnected pores. Moreover, the deformed HDPE matrix shrinks upon heating. As a result of the melting, PEO may, first, be redistributed in the pores of the matrix polymer and, second, because of the shrinkage, the subsequent crystallization may occur under conditions substantially different from the conditions of crystallization in the hybrid film. Therefore, only the processes of primary melting of PEO in the pores of matrix HDPE were studied in this work.

The study of melting the HDPE–PEO films has shown that the thermograms comprise two well-resolved endothermic peaks corresponding to HDPE and PEO melting, respectively, thereby indicating the phase separation of the components. When the solvent is removed, PEO crystallizes in the porous structure of deformed HDPE. The melting temperature and crystallinity of HDPE in hybrid film are 127 °C and 57%, respectively, and coincide with the data on the initial undeformed polymer. PEO crystallization in the nanoporous HDPE matrix is accompanied by a reduction in the melting temperature and crystallinity of PEO (Table 1) relative to PEO crystallized in bulk.

It should, once more, be noted that the pore length and width increase with the tensile strain of the polymer matrix.^{24,27}

Table 1. Thermophysical Properties of PEO (20 kDa) in HDPE–PEO Films

	PEO in HDPE–PEO films			PEO in bulk
	100	200	300	
tensile strain of HDPE, %	100	200	300	
PEO T_m , °C	60	60	61	65
PEO crystallinity, %	61	75	81	92

The changes in the pore sizes must, in turn, affect the process of PEO crystallization in HDPE nanopores, defectiveness of the formed crystals, and thermophysical characteristics of PEO in the HDPE films. Indeed, the lower the tensile strain of HDPE (i.e., the smaller the sizes of the confining space) upon the preparation of HDPE–PEO hybrid film, the greater the reduction in the crystallinity of PEO (Table 1). Thus, the spatial confinements of the nanoporous HDPE structure, which “hinder” PEO crystallization, lead to a decrease in the melting temperature and crystallinity of PEO in the film as compared with PEO crystallized in bulk. The result obtained agrees with the literature data on the influence of nanoscale spatial confinements on the crystallization and phase transitions of polymers.^{19,20}

The Study of PEO Structure in the Hybrid Films by FTIR Spectroscopy. The direction of PEO macromolecular chain orientation in hybrid films was studied by FTIR spectroscopy. The measurements were performed at polarization plane orientations parallel and perpendicular to the direction of polymer film stretching.

Figure 4a shows the spectra of the hybrid film resulting from HDPE stretching by 200% in PEO solutions. The difference is clearly seen between the spectra measured at polarization plane orientations parallel and perpendicular to the stretching direction. The optical densities of all HDPE–PEO films obtained by stretching HDPE to different tensile strains were measured for maxima of PEO absorption bands at 1242 cm^{-1} (complicated stretching and deformation vibrations of C–O–C groups), 1342 cm^{-1} (wagging deformation vibrations of methylene groups), and 1280 cm^{-1} (symmetric torsional vibrations of methylene groups), these bands being non overlapped with the bands of HDPE.

Figure 4b presents dichroic ratios as depending on the tensile strain of HDPE samples deformed in PEO solutions. At low tensile strains (below 130–150%), the bands at 1342 and 1242 cm^{-1} , which correspond to vibrations with dipole moments directed in parallel with the macromolecule axis PEO,²⁸ are more intense at the parallel orientation of the polarization plane ($A_{\parallel} > A_{\perp}$, $D > 1$) (Figure 4b, curves 1, 2). The band at 1280 cm^{-1} , which is relevant to variations in the dipole moment directed perpendicularly to the macromolecule axis,²⁸ is more intense when the polarization plane is perpendicular to the axis of HDPE stretching ($A_{\parallel} < A_{\perp}$, $D < 1$) (Figure 4b, curve 3). These data suggest that, in nanopores of crazed HDPE at low tensile strains, PEO macromolecular chains are predominantly oriented along (in parallel with) the stretching axis.

However, an opposite situation is observed at higher tensile strains (above 130% for the band at 1280 cm^{-1} or 150% for the bands at 1242 and 1342 cm^{-1}). The band at 1280 cm^{-1} is more intense ($A_{\parallel} > A_{\perp}$, $D > 1$), while the bands at 1342 and 1242 cm^{-1} are less intense ($A_{\parallel} < A_{\perp}$, $D < 1$) at the parallel orientation of the polarization plane, thereby indicating that the perpendicular orientation of the macromolecular chains prevails. The spectra measured upon the polarization plane rotation with a step of 15° for tensile strains of 75 and 300% indicate that the orientation varies gradually. Thus, the FTIR data show that HDPE–PEO hybrid films are characterized by orientation of incorporated PEO macromolecules. The direction orientation depends on pore sizes (or tensile strain of HDPE).

The Study of PEO Structure in the Hybrid Films by WAXS Analysis. The orientation of PEO macromolecular

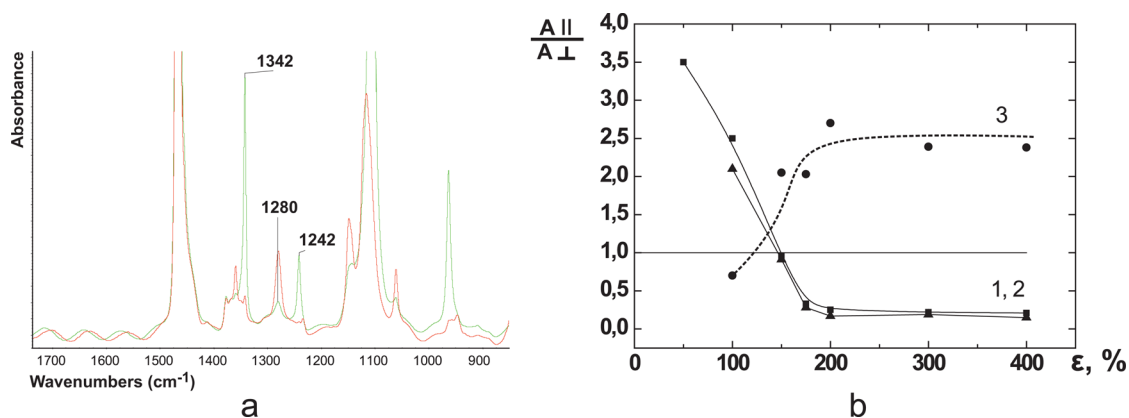


Figure 4. (a) FTIR spectra of HDPE–PEO film resulting from HDPE stretching by 200% in PEO solutions recorded at parallel (red line) and perpendicular (green line) orientations of polarization plane with respect to the stretching direction. (b) Dependences of dichroic ratios on the tensile strain of HDPE in HDPE–PEO films for PEO bands at (1) 1242, (2) 1342, and (3) 1280 cm⁻¹.

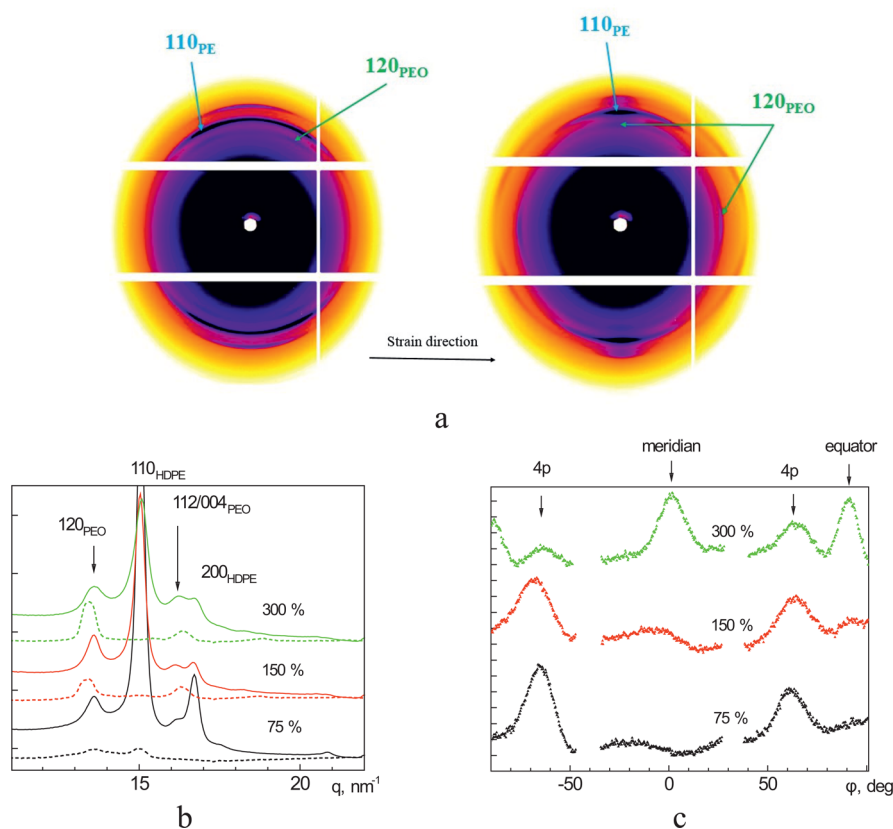


Figure 5. (a) X-ray scattering patterns of HDPE–PEO films for 75 (on the left) and 300% (on the right) tensile strains of HDPE stretched in the horizontal direction. (b) Corresponding diffraction patterns measured along the equatorial (solid curves) and meridional (dotted curves) directions for HDPE tensile strains of 75% (black), 150% (red), and 300% (green). The curves are shifted along the Y-axis for convenience. (c) Azimuthal intensity distributions of PEO reflection (120) for films resulting from HDPE deformation to different tensile strains: 75% (black), 150% (red), and 300% (green). The curves have been normalized relative to the background scattering and the scattering on HDPE. The zero angle corresponds to the meridional direction (the horizontal direction in the scattering patterns).

chains in HDPE–PEO films was also studied by WAXS. Figure 5a depicts the 2D X-ray diffraction patterns for samples obtained by stretching HDPE in PEO solutions to tensile strains of 75% (on the left) and 300% (on the right). In addition to HDPE reflections (110) and (200) at $q = 15$ and 16.7 nm^{-1} , the scattering curve exhibits PEO reflection (120) and overlapped reflections (112/004) at $q = 13.6$ and 16 nm^{-1} , which are inherent in the monoclinic structure of PEO.²⁹ Figure 5b illustrates the corresponding diffraction patterns in

the equatorial and meridional directions. An increase in the tensile strain causes a marked growth in the intensity of the PEO reflection (120) in the meridional region.

In order to analyze the texture and orientation of PEO crystallites in the hybrid films, the azimuthal intensity distribution curves were plotted for the reflection PEO (120) of samples with different tensile strains taking into account the instrumental scattering and the scattering on HDPE crystals (Figure 5c). The direction of the maximum growth of PEO

crystallites (direction 120) is perpendicular to the stretching direction. At a tensile strain of 75%, the four-point reflection (120) is predominantly observed with the intensity maximum at an angle of about 25° to the equator. This pattern is due to the presence of the row-texture of PEO with twisting around the b -axis perpendicular to the stretching direction and the pore axis. A similar scattering pattern was observed in,³⁰ however, the reflections were oriented at an angle of nearly 45° . The difference seems to be due to different types of the texture (row-texture in our case and multilayered structure in ref 30) resulting from different preparation procedures and crystallization conditions.

As the tensile strain is increased, the intensity of the four-point reflections, which were observed due to the population of crystallites with the row-texture at low tensile strains, gradually decreases, while reflections (120) arise in new azimuthal positions. For example, at 300% tensile strain, intense azimuthal reflections appear in the meridian, with these reflections corresponding to lamellae with c -axes of macromolecules perpendicular to the stretching direction. Moreover, equatorial reflections arise corresponding to lamellae with macromolecule c -axes parallel to the stretching direction.

Table 2 lists the fractions of PEO crystallites with different orientations in HDPE–PEO films as depending on the tensile

Table 2. Fractions of PEO Crystallites (%) with Different Orientations in HDPE–PEO Films As Depending on the Tensile Strain of HDPE

tensile strain, %	4-point reflection	equatorial reflection	meridional reflection
75	100	0	0
150	90	3	7
300	30	24	46

strain of HDPE. At 75, 150% tensile strains of HDPE, the fraction of PEO lamellae with c -axes of macromolecules oriented in parallel to the stretching direction and the row-texture is larger than 90%. An increase in the tensile strain leads

to the appearance of a substantial fraction (46%) of crystals with the perpendicular orientation of macromolecular chains.

Discussion of PEO Orientation in HDPE–PEO Films.

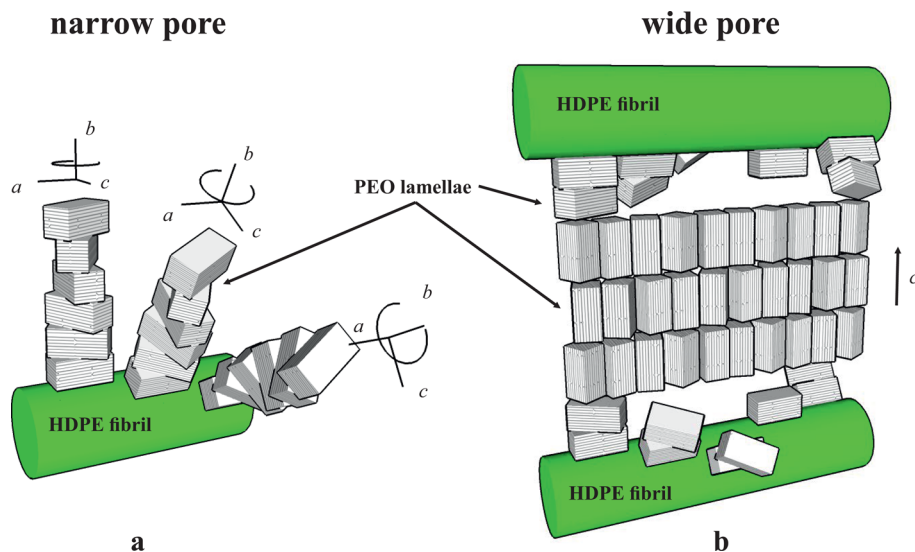
The fact that HDPE chains are oriented along the stretching axis in the course of crazing has been known previously.³¹ In this work, the orientation of PEO incorporated into HDPE nanopores has been revealed. The FTIR and WAXS analysis data show that, at low tensile strains of HDPE, PEO is orientated in HDPE–PEO films, with the c -axes of its macromolecules being parallel to the stretching axis; i.e., the edge-on lamella orientation with respect to fibrils and the direction of HDPE stretching takes place (Table 2). What is the reason for PEO orientation in HDPE–PEO films?

The crystallization is distorted in confined nanoscale volumes. Spherulites are degenerated into two-dimensional discoids or stacks of lamellae. Crystallization is often accompanied by orientation of lamellae under such conditions.^{14,15,17,21–23,32–34} It is obvious that the surface free energy for a surface formed by folds of macromolecules is substantially higher than that for a surface composed of densely packed mutually oriented molecules; i.e., the flat-on orientation of lamellae with respect to a substrate must dominate.

However, different orientations of lamellae may take place depending on the character of the interaction between a crystallizing polymer and a substrate, geometry of a confined space, and crystallization conditions. Obviously, the geometry and sizes of pores, which play the role of a confining factor, and the interaction between a crystallizing polymer and a substrate influence the processes of crystal nucleation and growth. In nanopores, the surface area-to-volume ratio of a pore is high; therefore, the surface nucleation is often observed on pore walls.¹⁰ The pore space in HDPE–PEO films is filled with nanofibrils that result from HDPE deformation by the crazing mechanism; therefore, PEO nucleation may occur on their surface. The nucleation on the fibril surface may be facilitated by PEO adsorption on HDPE fibrils, which precedes the crystallization (Figure 2a, curves 1, 3).

Moreover, in pores, the nucleation step prevails over the growth step, because the displacement of macromolecules to growing lamellae is “hindered” in the confined space. Thus,

Scheme 1. Schematic Representation of PEO Lamellae Orientation in HDPE–PEO Films at (a) 75 and (b) 300% Tensile Strains of HDPE



numerous nuclei are formed on HDPE fibrils, and these nuclei can grow, mainly, in the direction perpendicular to the fibrils, because their growth in the direction of a pore axis (along the fibrils) is limited by neighboring nuclei. An analogous situation has been observed in ref 35 for crystallization of macromolecules on nanofibers and nanotubes. The aforementioned factors seem to cause the formation of edge-on PEO lamellae at low tensile strains, with these lamellae growing perpendicularly to the pore walls (fibrils) and the stretching axis, while the *c*-axes of macromolecules being directed in parallel plane (Scheme 1a). In addition, the WAXS data (Figure 5) indicate that lamellae are twisting around the *b* axes to form a row-texture.

As the tensile strain of HDPE is increased when obtaining the hybrid films by crazing, the fraction of twisting lamellae with the row-structure (the four-point reflection) decreases. At the same time, edge-on lamellae with the *c*-axes directed in parallel with the pore walls but without twisting (equatorial reflections) and flat-on lamellae with the *c*-axes directed perpendicularly to the pore walls (meridional reflections) arise (Scheme 1b, Table 2). As can be seen from the table, the latter fraction composes almost a half of the total amount of the lamellae at high tensile strains. FTIR spectra actually show the overall orientation in a sample, i.e., the integral effect. Not all lamellae contribute to the FTIR spectra at the parallel orientation of the polarization plane because of twisting. Therefore, according to the FTIR data, lamellae with *c*-axes perpendicular to the stretching direction are, as a whole, prevailing at high tensile strains.

What is the reason for the appearance of lamellae with different orientations upon increasing tensile strain? As has been shown in the beginning of the article, at this geometry of the samples, the planar deformation of HDPE via the crazing mechanism is accompanied by disruption of HDPE lamellae. An increase in the tensile strain of HDPE causes pronounced fragmentation of lamellae and displacement of the fragments relative to each other. As a result, the length and width of the pores increase, and large, wide pores arise in addition to the narrow ones (Figure 1b). The dependence of orientation on the size of a nanopore in which crystallization occurs has been described in refs 10 and 22. It may be assumed that, twisting edge-on lamellae are present in narrow HDPE pores at both low and high tensile strains. As wide pores arise at high tensile strains (300%), edge-on PEO lamellae are formed at pore walls (on HDPE fibrils), as well as at low tensile strains, because the natures of the substrate and the crystallizing compound remain unchanged. However, these lamellae are not twisting because of the hindrance resulting from the formation of flat-on lamellae with the *c*-axes directed perpendicularly to the stretching direction in the pore space (Scheme 1b).

An increase in the pore length and width (pore volume) with a rise in the tensile strain changes the surface area-to-volume ratio of a pore; hence, the role of the surface in nucleation decreases. It is probable that, at high tensile strains in wide pores, the nucleation may occur both on the walls and in the volume of a pore;¹⁰ then, in addition to the edge-on lamellae with the parallel orientation of the *c*-axes, flat-on lamellae may grow with the *c*-axes perpendicular to the pore walls (Scheme 1b), as has been observed upon increasing pore size in ref 22.

Moreover, edge-on lamellae that have been formed at pore walls may serve as initiators for the growth of flat-on lamellae with their *c*-axes directed perpendicularly to the pore walls (fibrils) and the stretching axis. A similar situation has been

discussed in ref 32, in which defects of flat-on lamellae, such as lengthy loops, cilia, and screw-type dislocations, were considered to be the reasons for nucleation of edge-on lamellae. Thus, three types of PEO lamellae coexist in HDPE–PEO films at high tensile strains: in narrow pores, twisting edge-on lamellae with the *c*-axes directed in parallel with the pore walls (fibrils) and in wide pores, with edge-on lamellae without twisting and flat-on lamellae with their *c*-axes directed perpendicularly to the pore walls (fibrils) and the stretching axis.

CONCLUSIONS

Thus, crazing is an easy method to obtain hybrid materials based on polymers of different natures, such as hydrophobic HDPE and hydrophilic PEO, which is difficult to combine with traditional methods. Removal of a volatile liquid yields a hybrid films based on the deformed HDPE and PEO that has penetrated into the pores with the solvent. It is shown that stretching of HDPE films in PEO solution occurs by the mechanism of crazing (in this case ethanol acts as crazing agent) with the formation of fibrillar–porous structure. Parameters of the fibrillar–porous structure of crazes may be tuned by varying deformation conditions (tensile strains) of HDPE. In this regard, the influence of a fibrillar–porous structure of the HDPE matrix on the structure of incorporated PEO was considered.

The nanoporous structure of crazed HDPE in HDPE–PEO film predetermines the structure of incorporated PEO. Crystallization of PEO in HDPE matrix is accompanied by orientation and a reduction in the crystallinity and melting temperature of PEO. The reduction in the crystallinity and melting point of PEO in the hybrid films results from the spatial confinements created by the polymer matrix in the course of PEO crystallization; the smaller the pore sizes the greater the decrease in the crystallinity of PEO. The hybrid films are characterized by orientation of incorporated PEO, with the orientation being governed by variations in the conditions of PEO crystallization as depending on pore sizes.

The feasibility to craze various amorphous glassy and crystalline polymers makes it possible to consider crazing of polymers in solutions of high-molecular-mass compounds to be a simple and universal method for producing diverse polymer hybrid materials. The use of crazing as a method for the production of new polymer materials is advantageous in the fact that it enables one simultaneously to form a nanoporous structure of a matrix polymer, incorporate a second polymer into it, and distribute it uniformly to obtain a stable nanodisperse polymer material. Another advantage of crazing is the possibility of varying the sizes and morphology of pores. Thus, the results of this work show that the composition, orientation, and crystallinity of an incorporated component of a hybrid film obtained by the crazing method may be varied depending on the conditions of the crazing process.

AUTHOR INFORMATION

Corresponding Author

*(A.Y.Y.) E-mail: alyonussha@gmail.com.

ORCID

Alena Y. Yarysheva: 0000-0003-4997-6883

Notes

The authors declare no competing financial interest.

ACKNOWLEDGMENTS

This work was supported by the Russian Foundation for Basic Research, project No. 15-03-03430_a. We express our gratitude to the staff of a DIKSI station of the National Research Center Kurchatov Institute.

REFERENCES

- (1) Volynskii, A. L.; Bakeev, N. F. *Surface Phenomena in the Structural and Mechanical Behaviour of Solid Polymers*; Taylor & Francis: Boca Raton, FL, London, and New York, 2016; Chapter 6, 7.
- (2) Kausch, H. H.; Argon, A. S. *Crazing in Polymers*; Springer-Verlag: Berlin; New York, 1990, Vol. 2.
- (3) Kramer, E. J. Microscopic and molecular fundamentals of crazing. *Adv. Polym. Sci.* **1983**, 52-53, 1–56.
- (4) Rukhlya, E. G.; Litmanovich, E. A.; Dolinnyi, A. I.; Yarysheva, L. M.; Volynskii, A. L.; Bakeev, N. F. Penetration of Poly(ethylene oxide) into the Nanoporous Structure of the Solvent-Crazed Poly(ethylene terephthalate) Films. *Macromolecules* **2011**, 44, 5262–5267.
- (5) Trofimchuk, E. S.; Nikonorova, N. I.; Chagarovskii, A. O.; Volynskii, A. L.; Bakeev, N. F. Crystallization of Silver Chloride in Crazed Porous Polymers. *J. Phys. Chem. B* **2005**, 109, 16278–16283.
- (6) Toncelli, C.; Arzhakova, O. V.; Dolgova, A. A.; Volynskii, A. L.; Bakeev, N. F.; Kerry, J. P.; Papkovsky, D. B. Oxygen-Sensitive Phosphorescent Nanomaterials Produced from High-Density Polyethylene Films by Local Solvent-Crazing. *Anal. Chem.* **2014**, 86, 1917–1923.
- (7) Weichold, O.; Goel, P.; Lehmann, K.-H.; Möller, M. Solvent-Crazed PET Fibers Imparting Antibacterial Activity by Release of Zn²⁺. *J. Appl. Polym. Sci.* **2009**, 112, 2634–2640.
- (8) Steinhart, M. Supramolecular Organization of Polymeric Materials in Nanoporous Hard Templates. *Adv. Polym. Sci.* **2008**, 220, 123–187.
- (9) Liu, Y.-X.; Chen, E.-Q. Polymer crystallization of ultrathin films on solid substrates. *Coord. Chem. Rev.* **2010**, 254, 1011–1037.
- (10) Lee, K.; Yu, G.; Woo, E.; Hwang, S.; Shin, K. Freezing and Melting in Nanopores in Adsorption and Phase Behaviour in Nanochannels and Nanotubes; Dunne, L. J.; Manos, G., Eds.; Springer Science+Business Media B.V.: 2010, Chapter 12.
- (11) Li, H.; Yan, S. Surface-Induced Polymer Crystallization and the Resultant Structures and Morphologies. *Macromolecules* **2011**, 44, 417–442.
- (12) Lin, M.-Ch; Nandan, B.; Chen, H.-L. Mediating polymer crystal orientation using nanotemplates from block copolymer microdomains and anodic aluminium oxide nanochannels. *Soft Matter* **2012**, 8, 7306–7322.
- (13) Martín, J.; Maiz, J.; Sacristan, J.; Mijangos, C. Tailored polymer-based nanorods and nanotubes by "template synthesis": From preparation to applications. *Polymer* **2012**, 53, 1149–1166.
- (14) Carr, J. M.; Langhe, D. S.; Ponting, M. T.; Hiltner, A.; Baer, E. Confined crystallization in polymer nanolayered films: A review. *J. Mater. Res.* **2012**, 27, 1326–1350.
- (15) Wu, H.; Su, Z.; Takahara, A. Isotactic polystyrene nanorods with gradient crystallite states. *Soft Matter* **2012**, 8, 3180–3184.
- (16) Richard-Lacroix, M.; Pellerin, C. Molecular Orientation in Electrospun Fibers: From Mats to Single Fibers. *Macromolecules* **2013**, 46, 9473–9493.
- (17) Michell, R. M.; Blaszczyk-Lezak, I.; Mijangos, C.; Müller, A. J. Confinement effects on polymer crystallization: From droplets to alumina nanopores. *Polymer* **2013**, 54, 4059–4077.
- (18) Maiz, J.; Martín, J.; Mijangos, C. Confinement Effects on the Crystallization of Poly(ethylene oxide) Nanotubes. *Langmuir* **2012**, 28, 12296–12303.
- (19) Mandelkern, L. *Crystallization of Polymers*, 2nd ed.; Cambridge University Press: 2004.
- (20) Woo, E.; Huh, J.; Jeong, Y. G.; Shin, K. From Homogeneous to Heterogeneous Nucleation of Chain Molecules under Nanoscopic Cylindrical Confinement. *Phys. Rev. Lett.* **2007**, 98, 136103.
- (21) Michell, R. M.; Lorenzo, A. T.; Müller, A. J.; Lin, M.-C.; Chen, H.-L.; Blaszczyk-Lezak, I.; Martín, J.; Mijangos, C. The Crystallization of Confined Polymers and Block Copolymers Infiltrated Within Alumina Nanotube Templates. *Macromolecules* **2012**, 45, 1517–1528.
- (22) Wu, H.; Wang, W.; Huang, Y.; Su, Z. Orientation of Syndiotactic Polystyrene Crystallized in Cylindrical Nanopores. *Macromol. Rapid Commun.* **2009**, 30, 194–198.
- (23) Steinhart, M.; Senz, S.; Wehrspohn, R. B.; Gösele, U.; Wendorff, J. H. Curvature-Directed Crystallization of Poly(vinylidene difluoride) in Nanotube Walls. *Macromolecules* **2003**, 36, 3646–3651.
- (24) Yarysheva, A. Y.; Rukhlya, E. G.; Yarysheva, L. M.; Bagrov, D. V.; Volynskii, A. L.; Bakeev, N. F. The Structural Evolution of High-Density Polyethylene during Crazing in Liquid Medium. *Eur. Polym. J.* **2015**, 66, 458–469.
- (25) Bagrov, D. V.; Yarysheva, A. Y.; Rukhlya, E. G.; Yarysheva, L. M.; Volynskii, A. L.; Bakeev, N. F. Atomic Force Microscopic Study of the Structure of High-Density Polyethylene Deformed in Liquid Medium by Crazing Mechanism. *J. Microsc.* **2014**, 253, 151–160.
- (26) De Gennes, P. G. *Scaling Concepts in Polymer Physics*; Cornell University Press: Ithaca, NY, and London, 1979.
- (27) Arzhakova, O. V.; Dolgova, A. A.; Yarysheva, L. M.; Volynskii, A. L.; Bakeev, N. F. Development of a Stable Open-Porous Structure in the Solvent-Crazed High-Density Polyethylene. *Inorg. Mater.: Appl. Res.* **2011**, 2, 493–498.
- (28) Yoshihara, T.; Tadokoro, H.; Murahashi, S. Normal Vibrations of the Polymer Molecules of Helical Conformation. IV. Polyethylene Oxide and Polyethylene-d₄ Oxide. *J. Chem. Phys.* **1964**, 41, 2902–2911.
- (29) Takahashi, Y.; Tadokoro, H. Structural Studies of Polyethers, -(CH₂)_m-O-_n. X. Crystal Structure of Poly(ethylene oxide). *Macromolecules* **1973**, 6, 672–675.
- (30) Wang, H.; Keum, J. K.; Hiltner, A.; Baer, E. Impact of Nanoscale Confinement on Crystal Orientation of Poly(ethylene oxide). *Macromol. Rapid Commun.* **2010**, 31, 356–361.
- (31) Volynskii, A. L.; Bakeev, N. F. *Solvent crazing of polymers*; Elsevier: Amsterdam, New York, and Tokyo, 1995.
- (32) Wang, Y.; Chan, C.-M.; Ng, K.-M.; Li, L. What Controls the Lamellar Orientation at the Surface of Polymer Films during Crystallization? *Macromolecules* **2008**, 41, 2548–2553.
- (33) Shin, K.; Woo, E.; Jeong, Y. G.; Kim, C.; Huh, J.; Kim, K.-W. Crystalline Structures, Melting, and Crystallization of Linear Polyethylene in Cylindrical Nanopores. *Macromolecules* **2007**, 40, 6617–6623.
- (34) Wang, H.; Keum, J. K.; Hiltner, A.; Baer, E. Confined Crystallization of PEO in Nanolayered Films Impacting Structure and Oxygen Permeability. *Macromolecules* **2009**, 42, 7055–7066.
- (35) Abdou, J. P.; Reynolds, K. J.; Pfau, M. R.; van Staden, J.; Braggin, G. A.; Tajaddod, N.; Minus, M.; Reguero, V.; Vilatela, J. J.; Zhang, S. Interfacial Crystallization of Isotactic Polypropylene Surrounding Macroscopic Carbon Nanotube and Graphene Fibers. *Polymer* **2016**, 91, 136–145.